Hindawi
Advances in OptoElectronics
Volume 2018, Article ID 1262947, 8 pages
https://doi.org/10.1155/2018/1262947

*Research Article*

# Microfluidic Droplet Array as Optical Irises Actuated via Electrowetting

**Johannes Strassner, Carina Heisel, Dominic Palm, and Henning Fouckhardt**

*Integrated Optoelectronics and Microoptics Research Group, Physics Department, University of Kaiserslautern, P.O. Box 3049, 67653 Kaiserslautern, Germany*

Correspondence should be addressed to Johannes Strassner; strassner@physik.uni-kl.de

Received 6 October 2017; Accepted 17 December 2017; Published 1 February 2018

Academic Editor: Vasily Spirin



Initiated by a task in tunable microoptics, but not limited to this application, a microfluidic droplet array in an upright standing module with 3 × 3 subcells and droplet actuation via electrowetting is presented. Each subcell is filled with a single (of course transparent) water droplet, serving as a movable iris, surrounded by opaque blackened decane. Each subcell measures $1 \times 1\,\text{mm}^2$ and incorporates 2 × 2 quadratically arranged positions for the droplet. All 3 × 3 droplets are actuated synchronously by electrowetting on dielectric (EWOD). The droplet speed is up to 12 mm/s at 130 V ($V_{\text{rms}}$) with response times of about 40 ms. Minimum operating voltage is 30 V. Horizontal and vertical movement of the droplets is demonstrated. Furthermore, a minor modification of the subcells allows us to exploit the flattening of each droplet. Hence, the opaque decane fluid sample can cover each water droplet and render each subcell opaque, resulting in switchable irises of constant opening diameter. The concept does not require any mechanically moving parts or external pumps.

## 1. Introduction

Nowadays, technological progress is often inseparably linked to the miniaturization of electrical, mechanical, and optical components. Faster and more efficient processors, displays with increasing density of pixels, and new equipment for minimally invasive surgery are only a few prominent examples [1, 2].

Other developments are aimed at bringing complete chemical laboratory processes to the size of a chip. These so-called lab-on-a-chip devices allow for automatic analyses of small liquid samples [3].

In conventional lab chips continuous fluid flows are handled in microchannels. Hence, the degree of freedom of the fluid flow is small. Therefore, the functionality is completely determined by the chip design and prohibits alteration during operation. An alternative approach is made up of lab-on-a-chip devices for droplet manipulation (digital microfluidics, lab-on-a-chip 2.0). The droplets have volumes of a few pl to a few $\mu$l and can be moved more or less freely on the chip [4].

Some new microoptical devices are also based on droplet actuation. They often use the same droplet actuation principles as in digital lab chips. This way, pixels or displays [5–7], lenses [8], optical switches [9], optical attenuators [10], and others have been realized already.

The possibilities to actuate droplets are versatile and make use of the Marangoni effect [11], thermocapillarity [12], optical tweezers [13], dielectrophoresis [14], or electrowetting on dielectric (EWOD) [15], to name just a few.

EWOD is the most effective method, whenever a reliable way to electrically actuate discrete liquid droplets is sought after. The advantages of EWOD are relatively easy implementation, short response times, and low power consumption. Droplets can be created, moved, mixed, merged, and separated this way [16]. With an adequate arrangement of electrodes, it is also possible to control several droplets simultaneously.

In this contribution a device that allows for synchronous movement of a number of droplets—with a volume of just 60 nl each—is presented. The design of the droplet array, for example, also renders its application as an active microoptical pinhole array module possible [17].

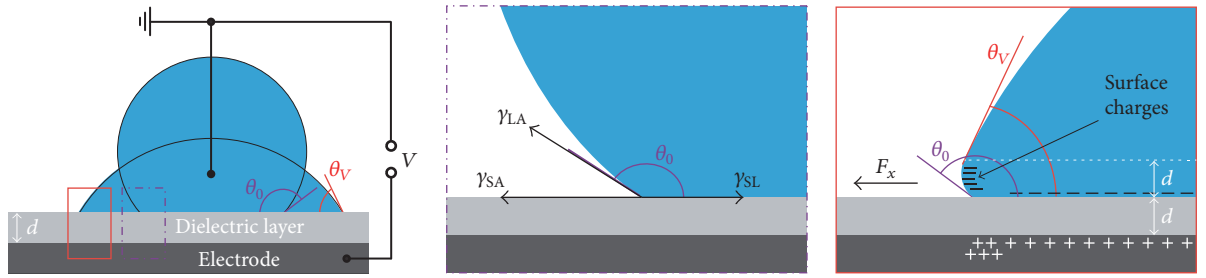


(a) (b) (c)

FIGURE 1: (a) Contact angle $\theta_0$ for zero voltage (violet) and $\theta_V$ for $V > 0$ (red). Microscopic view of the interface tension balance at the three-phase contact-line (TCL) (b) without voltage and (c) for a nonzero voltage.

## 2. EWOD Basics

A conductive droplet (like ionic water), which is separated from an electrode by a dielectric layer, keeps an equilibrium contact angle $\theta_0$ on the surface (see Figure 1(a)). This angle is determined by the force balance along the three-phase contact-line (TCL) that results from the surface tensions $\gamma_{ij}$ between solid (S), liquid (L), and ambient fluid (A: gaseous or liquid). The equilibrium contact angle $\theta_0$ can be derived by Young's equation (see also Figure 1):

$$\cos(\theta_0) = \frac{\gamma_{SA} - \gamma_{SL}}{\gamma_{LA}}. \quad (1)$$

If a voltage $V$ is applied between the conductive droplet and the electrode, the macroscopic contact angle will shrink. That is, the droplet spreads out and flattens. This phenomenon is called electrowetting on dielectric (EWOD). The contact angle $\theta_V$ under electrical bias can be derived by the Young-Lippmann equation [15]:

$$\cos(\theta_V) = \cos(\theta_0) + \frac{\varepsilon_0 \varepsilon_D}{2d \cdot \gamma_{LA}} \cdot V^2. \quad (2)$$

Here, $\varepsilon_0$ is the electric constant, $\varepsilon_D$ is the relative permittivity of the dielectric layer, and $d$ is its thickness.

An electromechanical simulation [18] reveals that, actually, the contact angle stays constant at $\theta_0$ in the direct vicinity of the surface of the dielectric layer, even in the presence of an electric field. Only at a distance from the surface of the dielectric layer, which is about equal to the thickness of this layer, the contact angle changes [19] (see Figure 1(c)) along the TCL due to strong Maxwell's mechanical stress caused by a high charge carrier density [18, 20].

By integrating Maxwell's stress over the TCL the electrostatic force $F$ acting on the droplet can be derived [18, 20, 21]. The surface-parallel component of the force acting on the droplet is [15, 20–22]

$$F_x = \frac{\varepsilon_0 \varepsilon_D}{2d} \cdot V^2 \cdot w. \quad (3)$$

Here, $w$ is the length of that part of the TCL that covers the electrode. Thus, the force moving the droplet depends on the kind and thickness of the dielectric layer, the applied voltage, and the length portion of the TCL above the electrode. Taking all these aspects into account, a chip that allows specific movement of any number of liquid droplets can be designed.

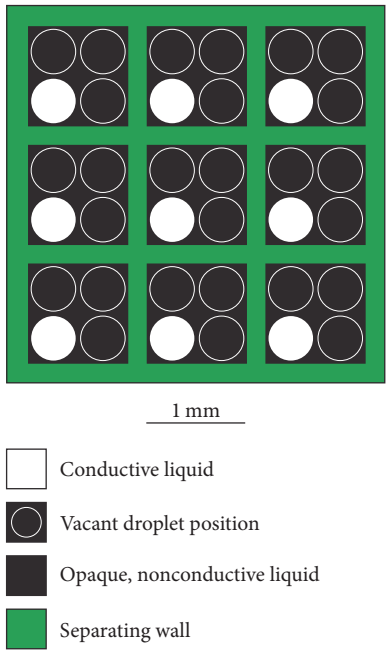


FIGURE 2: Schematic front-view of the array. Each of the 3 × 3 subcells contains a conductive water droplet in an opaque nonconductive ambient liquid. Each subcell allows for 2 × 2 droplet positions.

## 3. Design Concept

For test purposes, a 3 × 3 array/module has been envisaged. It consists of 3 × 3 separated subcells. Each of those is filled with a single conductive, transparent liquid droplet (here ionic water) surrounded by an opaque, nonconductive liquid (here blackened decane). The electrodes are arranged such that any of the 3 × 3 droplets can synchronously be moved into 2 × 2 distinct positions in each subcell, as sketched in Figure 2. A 3 × 3 array is chosen for a proof of concept, because it is the smallest array in which at least one subcell (the middle one) is completely enclosed/surrounded by others. Therefore, it can be assumed that the concept would also work for a larger array, if it worked for the 3 × 3 array.

The electrode design is depicted in Figure 3. Each subcell and the whole module require 2 × 2 distinct electrodes to

provide for 2 × 2 droplet positions. Our approach is to have two electrodes on the substrate (A, B) for droplet movement in the $x$-direction and two on the superstrate (C, D) for the $y$-direction. The chosen electrode arrangement prevents crisscrossing of the contact lines. Furthermore, it is possible to extend the array to a version with a nearly arbitrary number $X \times Y$ of subcells.

A jagged electrode design is used (see bottom of Figure 3). This ensures that in every position the droplet spatially extends to the adjacent electrode, allowing its movement into that direction.

Since there are actuation electrodes on both sub- and superstrates, the latter have both to be coated with the insulating dielectric material, namely, Parylene C from Specialty Coating Systems (SCS), Woking, UK. This procedure necessitates an additional (ground) contact for the droplet [10]. For symmetry reasons we used two ground contacts made from gold. The layer sequence is shown in Figure 4 together with the equivalent circuit diagram.

Using (of course transparent) ionic water as the conductive liquid and an opaque nonconductive ambient liquid, the chip could also be used as an optical aperture array. Our test array has 3 × 3 apertures/droplets with a fixed diameter of about 500 $\mu$m (related to the common volume of all droplets of 60 nl and the thickness of the cavity of about 250 $\mu$m). The droplets can synchronously be moved into 2 × 2 distinct positions each (see Figure 2) without any mechanically moving parts or external hydrodynamic pumps.

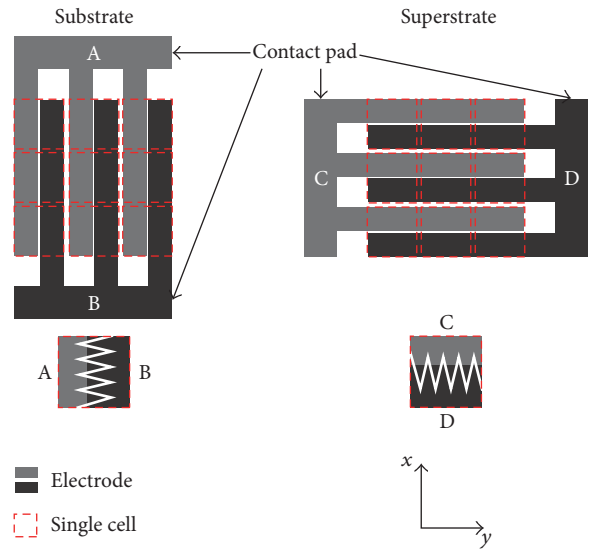


Figure 3: Schematic illustration of the electrode pattern. *Top*: overview with contact pads and positions of the individual subcells. *Bottom*: closer view of the electrode structure of a single subcell. The gap between two adjacent electrodes is zigzag-shaped (drawings not to scale).

## 4. Materials and Liquids

Water (deionized $H_2O$) with 0.1 wt.% NaCl is used as the transparent, conductive liquid. This is inexpensive and easy to prepare and to handle. The opaque, nonconductive liquid must be immiscible with water. Furthermore, it has to show a high optical attenuation. It surrounds the water droplet and fills the cell completely. The opaque liquid employed here is decane ($C_{10}H_{22}$) mixed with Solvent Black 3 ($C_{29}H_{24}N_6$, an oil dye purchased from Sigma Aldrich, Munich, Germany). The mixing ratio is 18.25 : 1; this corresponds to a dye concentration of 11.4 mmol/l.

For preparation, Solvent Black 3 is first dissolved in acetone. The solution is mixed with decane. After 2 h at 50°C on a hotplate, the solvent acetone has completely evaporated. The calculated spectrum of the optical attenuation of blackened decane (in dB per 100 $\mu$m absorption length) is depicted in Figure 5. The data are based on measured transmittance spectra, determined from blackened decane diluted in pure decane with a ratio of 1 : 100. A cuvette filled with pure decane was used for reference. The transmittance spectra were measured with a UV/VIS spectrometer (V670 from Jasco, Gross-Umstadt, Germany). Compared to mixtures of Solvent Black 3 in hexadecane [10], a more than twice as high attenuation is achieved over the entire wavelength range.

Parylene C is used as the dielectric material here. It is an inert, electrically and mechanically resistant, hydrophobic, and transparent material with high dielectric strength and thus is well suited for EWOD applications especially in optics. Compared to other works [9, 10, 23, 24], any hydrophobic surface coating has been omitted by us. The equilibrium contact angle of water (in air ambient) on Parylene C is (93 ± 5)°. In the configuration presented here, the droplets already move for AC voltages as low as $V_{\text{rms}} = 30$ V, even without additional hydrophobic coating. The omission of the coating and thus of common fluoropolymers (e.g., Teflon® AF or Cytop™) significantly simplifies processing and allows for even less expensive fabrication.

The material used for the transparent electrodes or contacts, respectively, on the sub- and superstrate is indium tin oxide (ITO, $In_2O_3$:$SnO_2$). Its transmission is 84% at 550 nm at the used layer thickness of 140 ± 20 nm, according to the manufacturer's specifications. A 17 $\mu$m wide gold wire is lithographically structured on each dielectric layer. It represents the ground electrode. To ensure a continuous contact to the droplet, the gold electrode is zigzag-shaped just like the gaps between the ITO electrodes (see Figure 3).

A 200 $\mu$m broad and 250 $\mu$m thick spacer structure made of Ordyl SY 355 defines the individual subcell areas. Ordyl is a dry film resist (from Elga Europe, Milano, Italy), which is applied to the substrate by hot-roll lamination and structured by photolithography. The thickness of the Ordyl film is about 50 $\mu$m. It is laminated onto the substrate in five layers here.

In the "open state" position, the irises have an insertion loss of approximately 0.65 dB at 570 nm and <1 dB averaged over the total visible spectrum. The on-off attenuation ratio of the irises is 30 dB at 570 nm and 15 dB averaged over the total visible spectrum.

## 5. Fabrication Technology

The individual fabrication steps are roughly illustrated with the sketches in Figure 6.

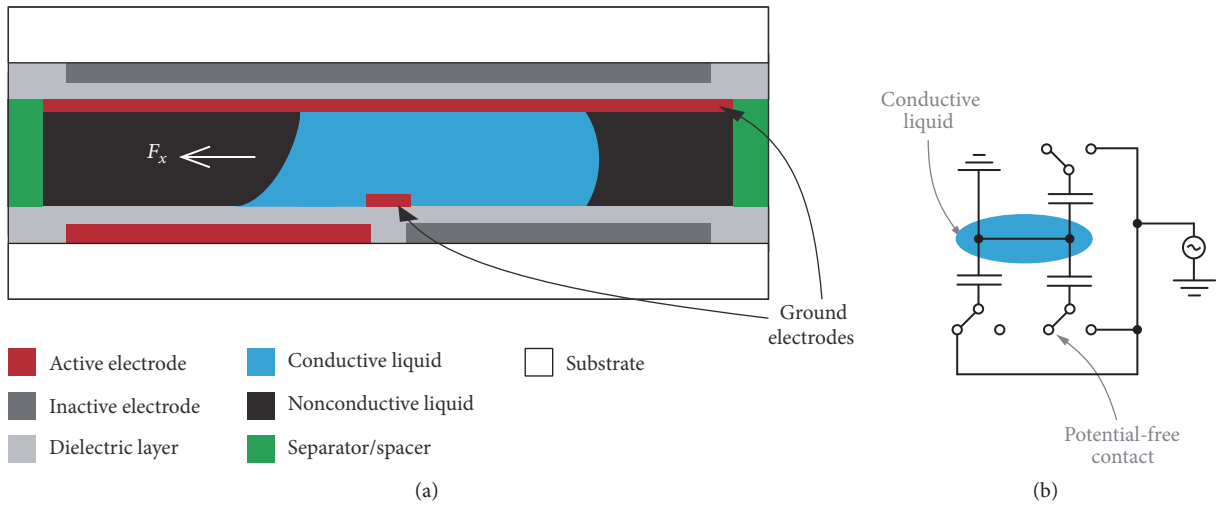


Figure 4: Cross-section of a single cell (not to scale (a)) and equivalent circuit diagram (b).

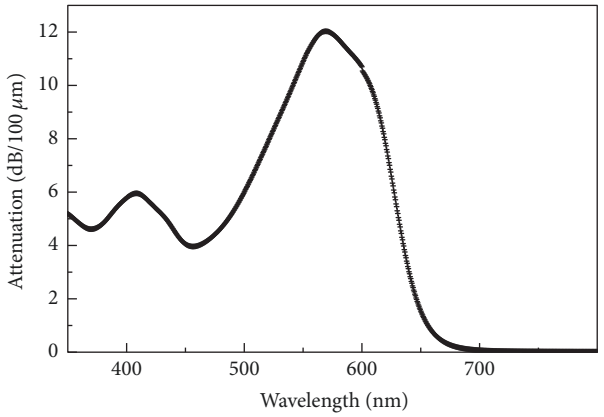


Figure 5: Optical attenuation (in dB per 100 $\mu$m absorption length) of Solvent Black 3 dissolved in decane.

ITO coated square glass slides have been purchased from Sigma Aldrich (product number 703192). The slide edge length is 25 mm and the thickness is 1.1 mm. In a first step, the electrodes are defined by photolithography. An image reversal photoresist (AZ 5214E from MicroChemicals, Ulm, Germany) is used as etch mask. Subsequently, the 140 nm thick ITO layer is wet-etched in hydrochloric acid (HCl, 32%, for 50 s). The etching is controlled by measuring the resistance between the two electrodes. The gap between the electrodes is 18 $\mu$m. To enable actuation/movement of the droplet from one electrode to the other, the electrodes are interlocked zigzag-shaped. In this way, the droplet always partially covers the neighboring electrode.

The 3.5 $\mu$m thick Parylene C layer is deposited by chemical vapor deposition (CVD). A PDS 2010 Parylene deposition unit from Specialty Coating Systems (SCS) is used. During this process, the powdery dimer dichloro-di(p-xylylene) is first vaporized at 175°C in vacuum and then pyrolized at 690°C. The resulting monomer chloro-p-xylylene condensates on the substrate at room temperature and forms a thin Parylene C polymer film. The film thickness is adjusted by the amount of initial loading of the dimer and is verified ex situ using a surface profilometer.

The gold ground electrodes are structured by a lithographic lift-off process. The negative photoresist AZ nLOF 2035 (MicroChemicals) is used for the mask. A chromium-gold layer sequence (a 10 nm thick chromium layer as adhesion promoter and a 200 nm thick gold layer) is deposited by electron beam deposition. The gold ground electrode is 17 $\mu$m wide. It follows the zigzag-shaped gap between the other electrodes to ensure persistent contact to each droplet.

The Ordyl layer stack (which serves as spacer and also defines the individual subcell areas; see Figure 6) is hot-roll laminated onto the substrate. Its total thickness is 250 $\mu$m after the fabrication process. The layer stack is UV-exposed, baked (3.5 min at 85°C), and subsequently developed.

The array structure is separated from broader spacer pillars in plane by a 1 mm wide gap. These spacings act as an overflow basin for the opaque liquid during chip bonding.

In a first step, the subcells are filled to about 75% with blackened decane by deposition of a drop with a coarse syringe. Then water droplets with a volume of 60 nl each are inserted into the subcells with a microliter syringe (7000.5 KH 0.5 $\mu$l from Hamilton, Reno, Nevada). After that the subcells are filled furthermore with opaque decane, until a meniscus forms over the entire array structure. The excess decane is pressed into the overflow basin upon bonding. This prevents encapsulation of air in the cells as much as possible. Sub- and superstrates are bonded with a MA/BA6 mask aligner (SUESS MicroTec, Garching, Germany) in bond aligner mode.

Figure 7 shows a photograph of the array structure with overflow basin of a fully assembled chip. The gold wires to ground the droplets can be seen as fine black lines. If the chip concepts were finally indeed be used for an optical module, the material of those electrodes would have to be changed from gold to a transparent conductive material like ITO again. But the chip presented here is a prototype just to show a proof of concept.

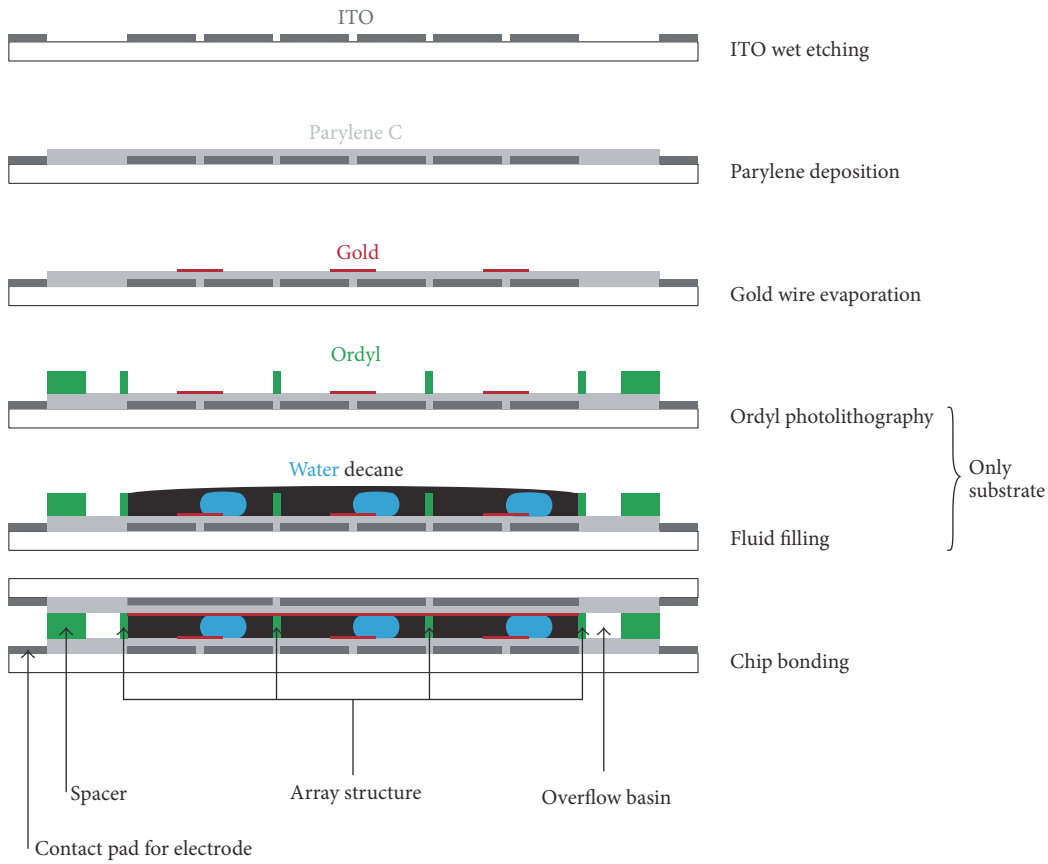


Figure 6: Illustration of the fabrication process of sub- and superstrate (not to scale).

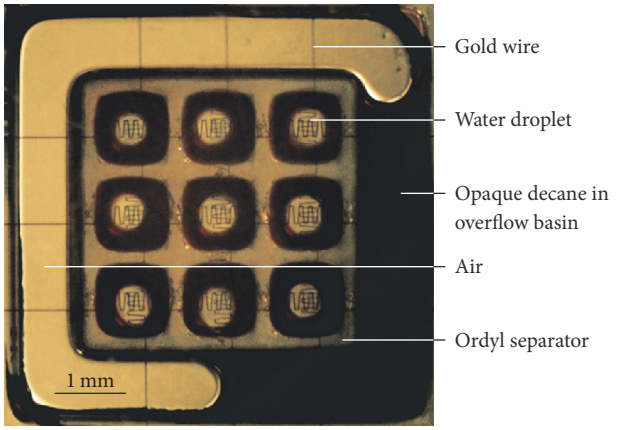


Figure 7: Photograph of the array structure with partially filled overflow basin. The droplets are in the center of the subcells, because, upon taking this photograph, the chip had just been finished and voltage had not yet been applied to the electrodes.

## 6. Actuation Setup

AC droplet actuation is chosen due to its many advantages over DC actuation, which are lower contact angle hysteresis, delayed contact angle saturation, and improved resistance to dielectric failure [10, 23]. Two power supplies, a pulse generator, and a high-frequency switch are used to generate a 5 kHz (called high-frequency here) AC voltage. The actuation setup used for droplet movement is depicted in Figure 8.

Two medium-voltage power supplies (type MCN 140–650 from FuG Elektronik, Schechen, Germany) generate a DC voltage. Power supply 1 provides for the negative polarity and power supply 2 for the positive one. The respective other pole is grounded. High-frequency switching between the two power supplies generates a square-wave output voltage. The switching frequency can be adjusted by a pulse generator (UPG 100 from ELV, Leer, Germany) to the before-mentioned 5 kHz. The HF switch is self-built. The rise time of the used MOSFET transistors (STP9NK60Z from STMicroelectronics NV, Geneva, Switzerland) is 17 ns and the fall time is 15 ns, the switching time of the HF switch is <50 ns. The square-wave voltage generated this way can be applied to each of the $2 \times 2$ electrodes via manual switches.

## 7. Results and Discussion

All droplets are moved synchronously to one of their $2 \times 2$ possible droplet positions depicted in Figure 2, due to the specific described electrode structure. Here, also a diagonal movement is possible.

Since the droplet diameter is below the capillary length of water, the influence of gravity on the droplet can be neglected

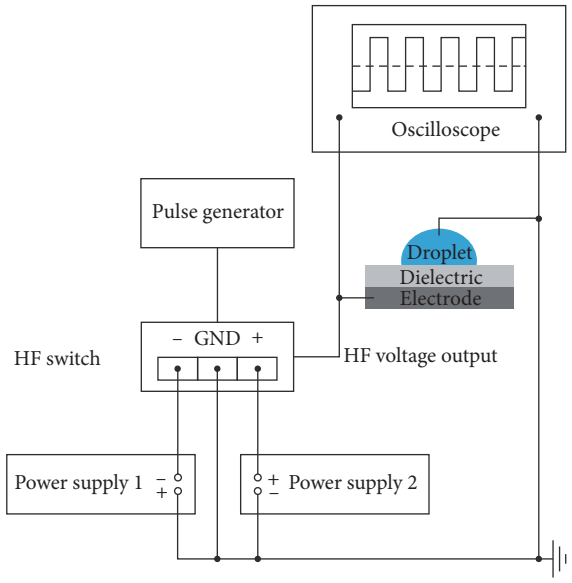


Figure 8: Setup for the generation of the high-frequency (5 kHz) square-wave voltage.

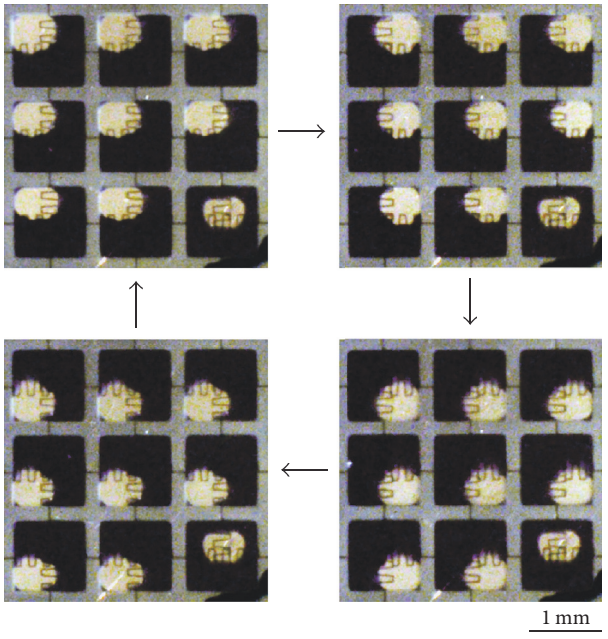


Figure 9: Video stills for the 2 × 2 droplet positions. The chip is mounted vertically. The bottom right droplet did not move or spread.

[25]. Images of an array that is standing upright with the droplets in the 2 × 2 different positions are shown in Figure 9.

In the video (Supplementary Material 1), the movement of the droplets at a driving voltage of $V_{rms}$ = 130 V at 5 kHz can be seen. A frame-by-frame analysis of the video reveals that most droplets can change the position in the time of capturing one frame by the other. At a frame rate of 24/s, this reveals a response time of about 40 ms and a translation speed of 12 mm/s.

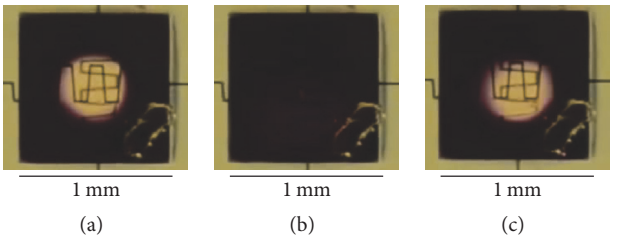


Figure 10: Photographs of a single subcell of an array, processed as a switchable iris, (a) without applied voltage, (b) with a voltage applied, and (c) relaxed droplet after voltage switch-off.

And a movement of the droplets can already be demonstrated at a voltage of $V_{rms}$ = 30 V. However, this results in a lower droplet velocity of 1.2 mm/s.

The bottom right droplet of the prototype module did not move or spread, probably due to a problem during assembly.

The chip presented here is a prototype module for a proof of concept. Based on the chip concept, for example, a microaperture array could be realized. As mentioned before, a transparent (ITO) electrode would then have to replace the gold ground contact for unhindered light transmission. Furthermore, in that case, the transparent Ordyl separator would have to be substituted by an opaque material, for example, by a structured silicon wafer (deeply reactive-ion etched) of appropriate thickness to prevent the transmission of light through the separators. Such a microaperture array could be applied, for example, in plenoptic cameras [17].

By a minor modification of the spacer height, the array can be used as a switchable pinhole array, not making use of the droplet movement, but of its (always occurring) flattening. The Ordyl spacer is laminated in ten instead of five layers, increasing the height of the spacer from 250 $\mu$m to 500 $\mu$m. In order to still ensure light transmission for the on-state of the aperture the droplet has to be in contact with sub- and superstrate. Thus, the droplet volume must also be increased from 60 nl to 160 nl. If a voltage of at least $V_{rms}$ = 100 V is applied to such an array, each transparent droplet will lose contact to the superstrate and will be flushed by the opaque liquid. Thus, the light path is blocked. A single subcell of such an array is shown in Figure 10 in action and as a video in Supplementary Material 2.

In this second application, the electrode on the substrate remains unstructured. The electrode on the superstrate can be, but does not have to be, omitted. The material under the superstrate remains Parylene C.

Similar concepts can be found in [26, 27], but we go a bit further here. The dark state in [23] is less homogenous and opaque. And the processing in [27] is more complex. In [28] the authors (including one of us) have presented an approach for a microfluidic iris array based on hydraulic pumping. The aperture is adjustable and the optical quality is excellent regarding vanishing wave-front distortion. Nevertheless, the space required for that module in $z$-direction is comparatively large and it needs an external pump, thus complicating integration in the existing systems. Our new concept has a compact design and no mechanically moving parts.

## 8. Conclusions

A proof of concept for the actuation of a droplet array has been presented, where a two-dimensional array of droplets can simultaneously be moved to four different positions using electrowetting on dielectrics (EWOD) as the actuation principle. The approach is almost arbitrarily extendable to larger arrays. The module has no mechanically moving parts (neglecting the droplets themselves). Furthermore, the size of the cells can be scaled in certain limits if needed. By minor modification of the design, the module may be manufactured using wafer-level fabrication.

## Conflicts of Interest

The authors declare that they have no conflicts of interest.

## Acknowledgments

This work has been funded by the German Research Foundation (DFG) under Contract FO157/45 within the framework of Priority Program 1337 "Tunable Micro-Optics." The authors would also like to thank the Nano Structuring Center of the University of Kaiserslautern for technical support and helpful discussions, Egbert Oesterschulze's research group for providing access to their Parylene coating unit, and Rolf Diller's research group for allowing access to its UV/VIS spectrometer.

## Supplementary Materials

*Supplementary 1.* A video that shows the movement of the droplets at a driving voltage of $V_{rms} = 130$ V at 5 kHz. A frame-by-frame analysis of the video reveals that most droplets can change the position in the time of capturing one frame by the other. At a frame rate of 24/s, this reveals a response time of about 40 ms and a translation speed of 12 mm/s. The bottom right droplet of the prototype module did not move or spread, probably due to a problem during assembly.

*Supplementary 2.* A video that shows a single subcell of a switchable pinhole array. By a minor modification of the spacer height, the array can be used as a switchable pinhole array, not making use of the droplet movement, but of its (always occurring) flattening.

## References

[1] U. Brinkschulte and T. Ungerer, *Mikrocontroller und Mikroprozessoren*, Springer, Heidelberg, Germany, 2010.

[2] C. H. B. Elliott and T. L. Credelle, "High-Pixel-Density Mobile Displays: Challenges and Solutions," *SID Symposium Digest of Technical Paper*, vol. 37, pp. 1984–1986, 2006.

[3] P. C. H. Li, *Microfluidic Lab-on-a-Chip for Chemical and Biological Analysis and Discovery*, CRC Press, Boca Raton, USA, 2005.

[4] Y. Fouillet, D. Jary, C. Chabrol, P. Claustre, and C. Peponnet, "Digital microfluidic design and optimization of classic and new fluidic functions for lab on a chip systems," *Microfluidics and Nanofluidics*, vol. 4, no. 3, pp. 159–165, 2008.

[5] S. Yang, K. Zhou, E. Kreit, and J. Heikenfeld, "High reflectivity electrofluidic pixels with zero-power grayscale operation," *Applied Physics Letters*, vol. 97, no. 14, Article ID 143501, 2010.

[6] R. A. Hayes and B. J. Feenstra, "Video-speed electronic paper based on electrowetting," *Nature*, vol. 425, no. 6956, pp. 383–385, 2003.

[7] B. Comiskey, J. D. Albert, H. Yoshizawa, and J. Jacobson, "An electrophoretic ink for all-printed reflective electronic displays," *Nature*, vol. 394, no. 6690, pp. 253–255, 1998.

[8] B. Berge and J. Peseux, "Variable focal lens controlled by an external voltage: an application of electrowetting," *The European Physical Journal E*, vol. 3, no. 2, pp. 159–163, 2000.

[9] C. Liu, L. Li, and Q. Wang, "Bidirectional optical switch based on electrowetting," *Journal of Applied Physics*, vol. 113, no. 19, p. 193106, 2013.

[10] P. Müller, A. Kloss, P. Liebetraut, W. Mönch, and H. Zappe, "A fully integrated optofluidic attenuator," *Journal of Micromechanics and Microengineering*, vol. 21, no. 12, Article ID 125027, 2011.

[11] K. T. Kotz, Y. Gu, and G. W. Faris, "Optically addressed droplet-based protein assay," *Journal of the American Chemical Society*, vol. 127, no. 16, pp. 5736-5737, 2005.

[12] A. L. Yarin, W. Liu, and D. H. Reneker, "Motion of droplets along thin fibers with temperature gradient," *Journal of Applied Physics*, vol. 91, no. 7, pp. 4751–4760, 2002.

[13] D. G. Grier, "A revolution in optical manipulation," *Nature*, vol. 424, no. 6950, pp. 810–816, 2003.

[14] K.-L. Wang, T. B. Jones, and A. Raisanen, "Dynamic control of DEP actuation and droplet dispensing," *Journal of Micromechanics and Microengineering*, vol. 17, no. 1, article no. 010, pp. 76–80, 2007.

[15] F. Mugele and J.-C. Baret, "Electrowetting: from basics to applications," *Journal of Physics: Condensed Matter*, vol. 17, no. 28, pp. R705–R774, 2005.

[16] S. K. Cho, H. Moon, and C.-J. Kim, "Creating, transporting, cutting, and merging liquid droplets by electrowetting-based actuation for digital microfluidic circuits," *Journal of Microelectromechanical Systems*, vol. 12, no. 1, pp. 70–80, 2003.

[17] A. Tuennermann, S. Gebhardt, and H. Fouckhardt, "Plenoptic Cameras," in *Tunable Micro-Optics*, H. Zappe and C. Duppé, Eds., Cambridge University Press, Cambridge, UK, 2015.

[18] J. Buehrle, S. Herminghaus, and F. Mugele, "Interface Profiles near Three-Phase Contact Lines in Electric Fields," *Physical Review Letters*, vol. 91, no. 8, 2003.

[19] F. Mugele and J. Buehrle, "Equilibrium drop surface profiles in electric fields," *Journal of Physics: Condensed Matter*, vol. 19, no. 37, p. 375112, 2007.

[20] K. H. Kang, "How electrostatic fields change contact angle in electrowetting," *Langmuir*, vol. 18, no. 26, pp. 10318–10322, 2002.

[21] T. B. Jones, "On the relationship of dielectrophoresis and electrowetting," *Langmuir*, vol. 18, no. 11, pp. 4437–4443, 2002.

[22] T. B. Jones, "An electromechanical interpretation of electrowetting," *Journal of Micromechanics and Microengineering*, vol. 15, no. 6, pp. 1184–1187, 2005.

[23] R. B. Fair, "Digital microfluidics: Is a true lab-on-a-chip possible?" *Microfluidics and Nanofluidics*, vol. 3, no. 3, pp. 245–281, 2007.

[24] M. G. Pollack, R. B. Fair, and A. D. Shenderov, "Electrowetting-based actuation of liquid droplets for microfluidic applications," *Applied Physics Letters*, vol. 77, no. 11, pp. 1725-1726, 2000.

[25] S. Hardt and F. Schönfeld, *Microfluidic Technologies for Miniaturized Analysis Systems*, Springer, New York, NY, USA, 2007.

[26] H. Ren, S. Xu, D. Ren, and S.-T. Wu, "Novel optical switch with a reconfigurable dielectric liquid droplet," *Optics Express*, vol. 19, no. 3, pp. 1985–1990, 2011.

[27] L. Li, C. Liu, and Q.-H. Wang, "Optical switch based on tunable aperture," *Optics Expresss*, vol. 37, no. 16, pp. 3306–3308, 2012.

[28] C. Kimmle, C. Doering, A. Steuer, and H. Fouckhardt, "Compact dynamic microfluidic iris array," in *Proceedings of the Optomechanics 2011: Innovations and Solutions*, USA, August 2011.